

Journal Pre-proofs

Review

Raster Scan optoacoustic Mesoscopy for detecting microvascular complications in diabetes mellitus: A narrative brief review

Dimitrios Pantazopoulos, Evanthia Gouveri, Vasilis Ntziachristos, Nikolaos Papanas

PII: S0168-8227(25)00109-3
DOI: <https://doi.org/10.1016/j.diabres.2025.112095>
Reference: DIAB 112095

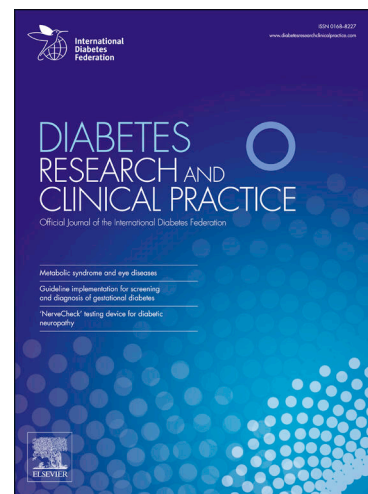
To appear in: *Diabetes Research and Clinical Practice*

Received Date: 28 January 2025
Revised Date: 25 February 2025
Accepted Date: 9 March 2025

Please cite this article as: D. Pantazopoulos, E. Gouveri, V. Ntziachristos, N. Papanas, Raster Scan optoacoustic Mesoscopy for detecting microvascular complications in diabetes mellitus: A narrative brief review, *Diabetes Research and Clinical Practice* (2025), doi: <https://doi.org/10.1016/j.diabres.2025.112095>

This is a PDF file of an article that has undergone enhancements after acceptance, such as the addition of a cover page and metadata, and formatting for readability, but it is not yet the definitive version of record. This version will undergo additional copyediting, typesetting and review before it is published in its final form, but we are providing this version to give early visibility of the article. Please note that, during the production process, errors may be discovered which could affect the content, and all legal disclaimers that apply to the journal pertain.

© 2025 Published by Elsevier B.V.



Raster Scan Optoacoustic Mesoscopy for detecting microvascular complications in diabetes mellitus: A narrative brief review

**Dimitrios Pantazopoulos,^{1,2} Evanthia Gouveri,² Vasilis Ntziachristos,^{1,3-5}
Nikolaos Papanas²**

¹Chair of Biological Imaging, Central Institute for Translational Cancer Research (TranslaTUM), School of Medicine and Health & School of Computation, Information and Technology, Technical University of Munich, Munich, Germany

²Diabetes Centre, Second Department of Internal Medicine, Democritus University of Thrace, Alexandroupolis, Greece

³Institute of Biological and Medical Imaging, Bioengineering Center, Helmholtz Zentrum München, Neuherberg, Germany

⁴Institute of Electronic Structure and Laser (IESL), Foundation for Research and Technology Hellas (FORTH), Heraklion, Greece

⁵Munich Institute of Biomedical Engineering (MIBE), Technical University of Munich, Garching b. München, Germany

Corresponding author: Dimitrios Pantazopoulos, Central Institute for Translational Cancer Research (TranslaTUM), School of Medicine and Health & School of Computation, Information and Technology, Technical University of Munich, Munich, Germany, dimitris.pantazopoulos@tum.de

Abstract

Diabetes mellitus (DM) may lead to microvascular and macrovascular complications. Screening for these complications is crucial and non-invasive methods with high-dissemination potential are needed. Diabetic peripheral neuropathy (DPN) is particularly challenging to screen due to the lack of reliable clinical markers and endpoints. In this context, Raster Scan Optoacoustic Mesoscopy (RSOM) emerges as a highly promising technique that offers hybrid, non-invasive imaging of optical absorption using light-induced ultrasound waves within tissue without the use of contrast agents. RSOM provides high-resolution visualisation of micro-vasculature, other tissue structures and functional information. The technique has already assessed microvasculature loss as a function of diabetes progression and used it to characterise DPN severity. RSOM has also

shown that cutaneous vessels in the mesoscopic range (mean diameters of 30-40 micrometers) are most prominently affected by DM and that the mean number of cutaneous vessels was lower in subjects with DM than in healthy participants ($p < 0.001$ and $p < 0.05$, respectively). Although experience is still limited, we present an overview of the novel technique in relation to its potential for detecting early DM onset and development of microvascular complications.

Key words: Diabetes, microvasculature, microvascular complications, diabetic peripheral neuropathy, optoacoustic imaging, raster scan optoacoustic mesoscopy

Introduction

Diabetes mellitus (DM) remains on the rise and is expected to affect over 575 million people by 2030 [1]. Similarly, the global prevalence of impaired glucose tolerance is increasing and is expected to reach 8.0% (454 million) by 2030 [1]. DM duration and hyperglycaemia represent the cardinal risk factors for the development of macrovascular complications [2-4]. Nevertheless, in contrast to macrovascular complications, recent evidence suggests that skin microangiopathy occurs early in the course of DM and may precede microvascular complications in other organs [5, 6]. This finding underlines the importance of detecting cutaneous microvascular perturbations early. Among non-invasive methods available to visualise microvasculature in vivo, optoacoustic mesoscopy stands out for its detailed imaging, providing high-resolution three-dimensional (3D) visualisation across the entire thickness of the epidermal and dermal layers [7-9].

Therefore, the aim of this narrative brief review was to discuss the potential use of the novel optoacoustic modality termed Raster Scan Optoacoustic Mesoscopy (RSOM) for imaging and detecting microvasculature damage across the DM spectrum, including prediabetes.

Search strategy

An electronic search was conducted in PubMed, EMBASE and Google Scholar using combinations of the following keywords: "optoacoustic mesoscopy," "photoacoustic imaging," "raster scan optoacoustic mesoscopy," "diabetes," "microvasculature damage," "microvascular complications." Optoacoustic imaging is also referred to as *photoacoustic* imaging. We retain the notation *optoacoustic* throughout this review, in analogy to all other *optical* imaging methods, such as *optical* microscopy,

optical spectroscopy, *optical* coherence tomography, etc., since it is the term *optical* that is used when employing light for visualisation or measurements. Nevertheless, we used both terms when searching the literature. All types of articles (reviews, original articles, clinical trials, case reports) in English were included. Articles in other languages were excluded. In addition, references of included articles were screened to identify additional relevant studies.

Microvasculature damage: what we know

The microvasculature includes blood vessels between first-order arterioles and first-order venules [2, 5, 10]. Arterioles and venules comprise endothelial cells, pericytes, a basement membrane (BM), and a layer of smooth muscle cells. Capillaries lack this smooth muscle layer [2, 5, 10].

Damage in the microvasculature begins early in DM and mainly affects the endothelial layer [2, 5, 10]. Indeed, it is now known that subjects with prediabetes may manifest early stages of chronic renal failure, diabetic neuropathy, retinopathy, or nephropathy [10-12]. Impressively, painful peripheral neuropathy has been reported in 8.7% of subjects with impaired glucose tolerance (IGT), compared with 4.2% in those with impaired fasting glucose (IFG) and 13.3% in those with DM [12]. Among adults with normoglycaemia, peripheral neuropathy is associated with increased all-cause mortality (hazard ratio [HR]: 1.37, 95% confidence interval [CI]: 1.21-1.55) and cardiovascular mortality (HR: 1.32, 95% CI: 1.02-1.72) [13].

Diabetic peripheral neuropathy

Diabetic peripheral neuropathy (DPN) remains one of the most frequent microvascular complications of DM. It is now increasingly appreciated that it may also present in some subjects with prediabetes [5, 6, 14]. DPN manifests in the distal lower extremities and primarily affects sensory modalities. Its progression is typically gradual over many years, though some individuals may experience a quicker and more severe course. Unfortunately, unlike nephropathy or retinopathy, DPN is challenging to screen for due to the absence of reliable clinical markers and endpoints for early detection or disease progression [6, 15-17].

One of the major suggested pathophysiological mechanisms of DPN is impaired blood flow in nerve microvasculature (*vasa nervorum*) with subsequent nerve ischaemic injury [18, 19]. Indeed, chronic hyperglycaemia affects endoneurial capillary morphology and endothelial cell function [18, 19]. The “neurovascular unit” is composed of neuronal, glial and vascular cells and is susceptible to biochemical alterations triggered by reactive metabolites and elevated glucose [20, 21]. Sural nerve biopsies from patients with DPN have demonstrated endoneurial basal membrane thickening along with endothelial cell proliferation and hypertrophy [6, 20, 21]. Such findings are generally absent in DM subjects without DPN [6, 20, 21].

With this in mind, it becomes evident that the need for early DPN diagnosis and timely intervention is essential. Significant progress has indeed been made in developing point-of-care diagnostic methods and devices, such as corneal confocal microscopy or automated nerve conduction study, as described in detail elsewhere [22-25].

Quantification of intra-epidermal nerve fibre density may be accomplished by distal leg skin biopsy, followed by immunohistochemistry and microscopic evaluation. This is considered by many the gold standard for assessment of small nerve fibres and early detection of subclinical neuropathy [26]. However, although this method is minimally invasive, it is still invasive, limiting its broader use as a diagnostic method. Corneal confocal microscopy (CCM) is non-invasive and studies small fibers in the cornea of the human eye [22, 23]. It has very good reproducibility and correlation with skin biopsy [22, 23]. However, CCM has inherent limitations. One of the main drawbacks is that CCM offers a small field of view (approximately $386 \times 386 \mu\text{m}$ per image or about 0.2% of the total subbasal nerve plexus) to achieve high resolution and magnification. This limitation necessitates multiple image acquisitions for comprehensive analysis, which can introduce variability and increase examination time [22, 23].

RSOM: a bit of light, a bit of (ultra)sound

To date, available techniques for assessing cutaneous tissue perfusion and oxygenation include Laser Doppler flowmetry, contrast-enhanced ultrasound, indocyanine green fluorescence angiography, near-infrared spectroscopy (NIRS) and others [27-30]. However, these modalities lack sufficient diagnostic value as they may lack sufficient resolution to visualize the microvasculature, average contributions from multiple skin layers and flow directions or require the injection of contrast agents [27-30]. Conversely, optoacoustic mesoscopy is a novel non-invasive technique providing high-resolution three-dimensional (3D) imaging under the skin surface, through the entire epidermal and dermal layers, as well as a detailed assessment of dermal microvasculature and other skin features [31]. Moreover, it does not require administration of contrast agents [31].

Optoacoustic imaging, in general, is an optical imaging technique illuminating tissue with transient light energy, such as photon pulses in the nanosecond range [32]. When different tissue molecules absorb the excitation light, absorption causes rapid thermoelastic expansion at the absorption sites. This expansion produces ultrasound waves, which travel through the tissue and are detected by ultrasound sensors placed at various points on the tissue surface. A time-dependent ultrasound signal is captured at each detector position: the signals recorded later originate from deeper layers within the tissue, while earlier signals originate from shallower regions. By processing all recorded signals from each position with image reconstruction techniques, detailed images based on optical absorption within the tissue can be created [33-38]. Use of ultrasound detectors rather than optical cameras enables imaging with high resolution and high optical contrast [39, 40].

Most clinical studies using optoacoustic imaging have concentrated on detecting intrinsic contrast in the visible or near-infrared range (NIR), enabling the identification of contrast from natural tissue chromophores (i.e. water, lipids, haemoglobin, melanin). NIR is ideal for imaging through several centimetres of tissue due to the low tissue absorption of light in this wavelength range [41, 42]. Conversely, imaging in the visible light range can only penetrate a few millimetres due to the high absorption of light by haemoglobin. However, this low penetration is balanced by the enhanced contrast achieved when imaging blood vessels over other spectral regions and the achieved contrast is generally better than other imaging modalities. Therefore, imaging of cutaneous microvasculature can be achieved with high contrast in the visible range since haemoglobin is a highly potent light absorber and generates strong optoacoustic signals.

In addition to the dependence of optical absorption on wavelength, optoacoustic imaging also offers a trade-off in terms of the ultrasound frequency utilised [7]. Specifically, the image resolution improves when a higher frequency is used, allowing for finer detail, but the imaging depth decreases due to the steeper attenuation of higher ultrasound frequencies as a function of propagation distance [43]. Conversely, the detection of lower ultrasound frequencies allows for greater imaging depth but reduces the level of detail, resulting in lower resolution. Therefore, for macroscopy applications at depths of a few centimetres (**Table 1**), the NIR region is matched to ultrasound frequencies of 0.1-10 Mhz. On the contrary, ultrasound frequencies >10 MHz, as applicable to optoacoustic mesoscopy and microscopy, are matched to illumination in the visible range to yield images with high resolution and high contrast from the vasculature or the melanin layer [43, 44].

Therefore, high-resolution imaging of the skin, including cutaneous microvasculature can be achieved by recording signals at frequencies ranging from a few tens of MHz up to more than a hundred MHz. While frequencies at the few tens of MHz yield mesoscopic resolutions at several tens of micrometers, the use of an extended frequency range to more than 100Mhz allows resolutions in the few tens of micrometers or better, therefore reaching microscopic imaging. To achieve such high-bandwidth detection, RSOM utilises broad-band single-element detectors, which are raster scanned across the skin (**Figure 1**) [37, 39]. RSOM achieves sub-10 micrometer resolutions and enables visualization much deeper than optical microscopy methods, reaching depths that allow visualisation of microvasculature over the entire dermal layer. Moreover, by illuminating at multiple wavelengths, it is possible to separate the contributions of oxygenated and deoxygenated haemoglobin and determine oxygen saturation (SO_2) levels in tissues and microvessels [39, 43-45].

Through analysis of the microvasculature patterns revealed by RSOM (**Figure 1**), it is possible to compute vascular dilation and total blood volume, which are label-free markers for inflammation. RSOM has demonstrated its potential as an imaging method in various clinical settings, such as psoriasis [7, 46], atopic dermatitis [47, 48], melanoma [49, 50], and microvascular complications of DM [51, 52]. **Table 1** summarises some of the characteristics of aforementioned optoacoustic imaging modalities and their main applications.

RSOM and diabetes: where do we stand?

Experience on the use of RSOM for early detection of microvascular dysfunction in DM comes from two clinical studies conducted by teams under the leadership of Professor Ntziachristos, as summarised in **Table 2**.

He et al. [51] employed ultra-wideband RSOM (UWB-RSOM) to assess the impact of DM on the skin, providing novel *in vivo* insights into how dermal and epidermal characteristics relate to diabetes-associated complications. This study included 95 subjects with DM (both type 1 and 2) and 48 healthy volunteers without DM. Mean DM duration was 20 ± 16 years and mean glycated haemoglobin (HbA_{1c}) was $7.1 \pm 1.1\%$. [51]. Participants with DM were further divided into 3 subgroups: 1) DM and no complications ($n = 45$, no DPN and no atherosclerotic cardiovascular disease [ASCVD]), 2) DM with DPN but no ASCVD ($n = 25$), 3) DM with DPN and ASCVD ($n = 25$) [51].

Measurements were performed in the supine position [51]. RSOM illuminated at 532 nm (green) and scanned with an ultrasound transducer with bandwidth ranging from 10 to 120 MHz and a central frequency of 50 MHz over a 4×2 mm² field of view. Each participant was scanned at 2 symmetric regions over the pretibial region of the distal lower limb [51].

To quantify the differences observed through visual inspection of the RSOM images and to extract relevant label-free RSOM biomarkers, researchers designed an RSOM image analysis pipeline. Based on this, 6 specific RSOM image features were analysed. In the dermal layer, these features were: 1) total number of smaller vessels (<10 - 40 μm), 2) total number of larger vessels (40 - 150 μm), 3) total vessel number and 4) total blood volume. The remaining two features were 5) epidermal thickness and 6) epidermal signal density [51]. The 40 μm threshold is commonly used to distinguish small arterioles and venules from larger or smaller capillaries (5 - 10 μm). Smaller vessels (<40 μm) are located within the epineurium and endoneurium (vasa nervorum) and their ischaemic changes represent an underlying mechanism of DPN [63-65].

In healthy skin, RSOM revealed dense signals from the epidermal layer along with a vascular network in the dermal layer, featuring numerous blood vessels of varying diameters. In contrast, participants with DM exhibited significantly reduced dermal vessel density, with a distinct high-contrast boundary between the epidermal and dermal layers. Total vessel count was 16.87 ± 9.30 in DM participants vs. 30.12 ± 9.87 in healthy volunteers ($p < 0.01$) [51]. Smaller vessels were 2.8 times fewer in the DM group than in volunteers (3.45 ± 2.62 vs. 9.78 ± 3.41 vessels, $p < 0.001$). The same was observed for larger vessels, with a mean of 13.39 ± 11.30 vessels DM group compared with 20.34 ± 8.32 vessels ($p < 0.05$). Analysis of the epidermal layer also showed significant differences between the two groups. Mean epidermal thickness was 105.27 ± 17.04 μm in healthy volunteers vs. 81.03 ± 23.06 μm in participants with DM ($p < 0.05$). Additionally, the signal density of the epidermal layer, reflecting contributions from melanin and capillaries, was significantly lower in DM participants ($p < 0.05$) [51].

These researchers [51] also investigated the relationship between DPN and RSOM-derived data. To this purpose, they analysed RSOM features from participants with DM without complications, as well as those with varying severity of DPN. Severity of neuropathy was assessed clinically using the Neuropathy Disability Score (NDS) and the Neuropathy Symptom Score (NSS). DM participants were divided into 3 categories: no complications (NC, $n = 45$), low-score neuropathy (LN, $n = 13$; $1 \leq \text{NDS} \leq 5$ or $1 \leq \text{NSS} \leq 5$), and high-score neuropathy (HN, $n = 12$; $\text{NDS} > 5$ or $\text{NSS} > 5$). RSOM images revealed a progressive decrease in vascular density in the dermal region with increasing DPN severity. The number of small vessels showed significant differences between the 3 DM groups, with comparisons of healthy vs. NC ($p < 0.01$), NC vs. LN ($p < 0.05$), and LN vs. HN ($p < 0.001$). Healthy subjects exhibited the highest number of small vessels, and this number became progressively smaller with increasing severity of DPN [51].

He et al. [51] also analysed data between subjects with DPN and ASCVD ($n=25$) and those with DPN alone ($n=25$). Significant differences were observed in the numbers of small, large, and total vessels between the group with and the group without atherosclerosis. Fewer small vessels were seen in participants with DPN and ASCVD than in those with DPN alone [51]. The number of small vessels exhibited the most significant difference ($p < 0.001$), followed by the number of total vessels ($p < 0.01$) and the number of large vessels ($p < 0.05$), suggesting its potential as a differentiating biomarker between healthy subjects and those at various stages of DM complications [51].

In the other study, Karlas et al. [52] demonstrated that morphophysiological characteristics obtained from RSOM images can link skin microangiopathy phenotypes with DM complications. A clinically interpretable Artificial Intelligence (cxAI) approach was applied to RSOM skin images with the aim of linking skin characteristics with diabetes-related complications [52]. They obtained 199 RSOM images from 115 participants (40 healthy and 75 with type 1 or type 2 DM). Participants with DM were further divided into 3 subgroups: 1) group A: DM without complications (DPN or ASCVD), 2) group B: DM and either DPN or ASCVD, and 3) group C: DM with both DPN and ASCVD [52]. Participants were scanned with the RSOM system described before over the distal anterolateral region of the dominant leg (~15 cm above the ankle joint). Using cxAI, 32 explainable features were identified. These were further categorised into 3 scales of architectural detail: the microscale ($< 100 \mu\text{m}$), the mesoscale ($\approx 100\text{-}1,000 \mu\text{m}$) and the macroscale ($> 1,000 \mu\text{m}$). The mesoscale, which defines the structure and arrangement of the microvascular network, (for example number of vessels in the dermal layer, number of junction-to-junction branches in the dermal layer) was more affected by presence of DM and its complications (DPN and ASCVD) compared with microscale and macroscale features [52]. The most noticeable changes associated with presence of diabetic complications included 1) a reduction in the number of junction-to-junction dermal layer branches, 2) a consistent increase in the number of vessels in the epidermal layer, and 3) a steady decrease in the number of junction-to-junction dermal layer branches [52].

Karlas et al. [52] also combined the aforementioned 32 skin features into a single “microangiopathy score”. This score demonstrated an ability to distinguish DM participants from volunteers with an area under the receiver operating characteristic

(ROC) curve (AUC) of 0.84, showing 80% sensitivity and 78% specificity. The “microangiopathy score” of DM subjects (0.76 ± 0.13) was higher than that of healthy volunteers (0.56 ± 0.16), ($p < 0.001$) [52]. This difference remained significant after controlling for age, suggesting a potential utilisation of RSOM for differentiating healthy individuals from subjects with DM [52].

Discussion

Microvascular complications of DM develop due to increased oxidative stress, i.e. through the accumulation of reactive oxygen species (ROS) and enhanced inflammation [63-66] and increase morbidity [65, 66]. Given that microvascular changes may develop early, before the onset of clinical symptoms [2, 66], they could be used to monitor the onset of DM and its complications.

Microvascular complications similar to those of diabetic retinopathy and diabetic kidney disease may also develop in the skin [67, 68]. Moreover, the skin may contribute to their timely detection by virtue of being the largest and most accessible organ of the human body. Therefore, the development of modalities that can accurately capture the cutaneous micro-vascularisation may enable novel diagnostic and theranostic abilities in DM detection and management.

The importance of skin as a diagnostic window in DM has been demonstrated through the use of photoplethysmography (PPG) [69]. PPG primarily captures signals related to blood volume changes in the microvascular bed, influenced by arterial pulsations. Although PPG does not directly measure the skin, its signals are acquired through it, with their quality impacted by skin condition and optical properties. In diabetes, PPG captures heart rate, heart rate variability (HRV), and waveform morphologies, offering insights into diabetic vascular changes such as endothelial dysfunction and arterial stiffening [69-71].

In this context, RSOM has the potential to offer information on early microvascular changes in the skin and possibly contribute to detection of diabetic complications [51, 52]. With a combination of strong contrast from haemoglobin, tissue penetration that goes far beyond optical microscopy and superb three-dimensional resolution due to wide bandwidth, RSOM is an ideal modality for detailed three-dimensional visualization of cutaneous microvasculature. RSOM further achieves resolution in few tens of micrometers or better along all three geometrical dimensions. Therefore, it is the only modality that has demonstrated high-resolution cross-sectional images of the skin *in vivo*. This unique performance opens up new possibilities for exploring cutaneous features in 3 dimensions and provides innovative approaches for disease detection through the skin, surpassing what can be achieved with traditional superficial examination techniques. Additionally, the detailed images produced by RSOM can facilitate precise analytics through computational image analysis tools, enabling quantification of microvascular changes and other morphological features [52].

From a practical point of view, RSOM is already commercially available, with a cost around 200000 Euros, which is expected to substantially decrease during the next years. This renders it easily accessible for research and potential clinical applications. As technology evolves, its integration into routine diagnostic workflows may become more feasible, further enhancing its cost-effectiveness over time [72]. Moreover, RSOM is a user-friendly imaging modality that does not require specialised engineering or technical expertise, making it accessible to clinicians. After an initial familiarisation period with the device, system interface, and software, users can quickly achieve high-quality measurements. With continued use, proficiency improves, allowing for efficient data acquisition and interpretation. While no formal studies have quantified the learning curve, experience suggests that clinicians can reliably use RSOM after a relatively short period of hands-on practice. Its operation ensures that, beyond basic training, no extensive technical background is required for effective use in a clinical setting. Additionally, although there are no formal studies on the reproducibility of RSOM, the modality's high-resolution imaging and consistent technology suggest that it may provide reliable results across different users and settings. Naturally, as with any imaging technique, reproducibility is influenced by operator skill and device calibration. However, given its straightforward operation and minimal technical demands, RSOM is expected to demonstrate a high degree of reproducibility once proper protocols are established.

Therefore, RSOM may offer several key advantages in the study and clinical management of DM. First, it provides non-invasive, portable, high-resolution imaging of skin microvasculature and tissue structure without the need for contrast agents. Secondly, RSOM has shown the potential of not only differentiating healthy individuals from subjects with DM, but also of using objective and quantifiable cutaneous features as biomarkers of the onset of DM and its complications. Furthermore, its ability to integrate functional and morphological data represents an opportunity to study the evolution of microvascular perturbations, increasing our understanding of their pathogenesis.

A further potential implication of RSOM in the future might be the study of neo-vascularisation in patients with diabetic foot ulcers (DFUs). It has already been shown that the lowest density of small vessels was observed in the presence of advanced DPN [51], which is a recognised risk factor of DFUs [4, 19]. It remains to be shown whether RSOM findings of reduced neo-vascularisation suggest a risk of poor DFU healing and whether this knowledge might be of relevance for patient treatment and monitoring.

Moreover, it is well established that genome-wide association studies have identified (and continue to identify) independent genetic loci associated with type 2 DM and its microvascular complications [73, 74]. Therefore, work is progressing on using RSOM within a framework for early damage detection for DM prevention by combining optoacoustic phenotypes with specific genotypic and multi-omic analyses.

However, RSOM has some limitations. Currently, available data originate from only two single-centre studies with a limited number of patients. Larger, multi-centre studies or works from additional centres are necessary to generate new, more comprehensive data. Moreover, skin changes have only been correlated with DPN. Thus,

it would be useful to correlate RSOM findings with retinopathy and chronic kidney disease (CKD), each with its own staging systems. Such data will enable a more thorough insight into the development and progression of microvascular disease in DM. Finally, no studies have yet compared RSOM with other diagnostic methods, such as corneal confocal microscopy or skin biopsy, in detecting microvascular complications in diabetes. Such studies will contribute towards ascertaining the comparative diagnostic value of RSOM.

In conclusion, assessment of skin microvasculature could lead to a novel means of monitoring the onset of DM and its complications, as well as or development of vascular complications, allowing quantification of the true burden of the disease on the vascular system rather than disease course predictions offered by risk factors. A non-invasive, portable, and label-free technology like RSOM could be essential for providing quantitative metrics in high-risk populations and assessing potential interventions and in prevention programmes.

Conflicts of interest: **Dimitrios Pantazopoulos** has been supported by Technical University of Munich. **Evanthia Gouveri** has attended conferences sponsored by Berlin-Chemie, Sanofi, AstraZeneca, Novo Nordisk, Lilly and Boehringer Ingelheim; received speaker honoraria by Boehringer-Ingelheim, Sanofi and Menarini. **Nikolaos Papanas** has been an advisory board member of Astra-Zeneca, Bayer, Boehringer Ingelheim, Menarini, MSD, Novo Nordisk, Pfizer, Takeda and TrigoCare International; has participated in sponsored studies by Astra-Zeneca, Eli-Lilly, GSK, MSD, Novo Nordisk, Novartis and Sanofi-Aventis; has received honoraria as a speaker for Astra-Zeneca, Bayer, Boehringer Ingelheim, Eli-Lilly, Elpen, Menarini, MSD, Mylan, Novo Nordisk, Pfizer, Sanofi-Aventis and Vianex; and has attended conferences sponsored by TrigoCare International, Eli-Lilly, Galenica, Menarini, Novo Nordisk, Pfizer and Sanofi-Aventis. **Vasilis Ntziachristos** is a founder and equity holder of iThera Medical GmbH, Spear UG, sThesis GmbH, I3 Inc and Maurus OY.

Acknowledgments: This project has received funding from the European Union's Horizon 2020 research and innovation programme under grant agreement No 101017802 (OPTOMICS).

Table legends

Table 1. Optoacoustic imaging modalities.

Table 2. Clinical studies of Raster Scan Optoacoustic Mesoscopy in DM.

Figure legend

Figure 1. a) Setup for Raster-scan Optoacoustic Mesoscopy (RSOM). Controller: Motion controller for motorised stages, PC: Computer. b) RSOM's principle of operation. After affixing the handheld probe to the skin surface, light is pulsed repeatedly to excite ultrasound (US) waves within tissue while the ultrasound detector is moved in a raster pattern along the XY plane to collect ultrasound signals emitted by absorbers. The ultrasound waves are then used to mathematically reconstruct images of the optical contrast that produced them. ED: epidermal layer, DE, dermal layer. c) A one-dimensional (1D) ultrasound signal is recorded by the detector at each scanning point (green circle) for each light pulse. d) The recorded 1D ultrasound signals are then

reconstructed into a volumetric three-dimensional (3D) image. High-frequency (green) or low-frequency (red) signals show the finer or coarser vasculature, respectively. The epidermal/ subpapillary vascular plexus is found between the white dotted lines. Adapted from Karlas et al. under a CC-BY 4.0 license [Karlas A et al. Dermal features derived from optoacoustic tomograms via machine learning correlate microangiopathy phenotypes with diabetes stage. *Nat Biomed Eng* 2023;7(12):1667-1682].

References

1. Saeedi P, Petersohn I, Salpea P, et al. Global and regional diabetes prevalence estimates for 2019 and projections for 2030 and 2045: Results from the International Diabetes Federation Diabetes Atlas, 9th edition. *Diabetes Res Clin Pract* 2019;157:107843.
2. Chawla A, Chawla R, Jaggi S. Microvascular and macrovascular complications in diabetes mellitus: Distinct or continuum? *Indian J Endocrinol Metab* 2016;20(4):546-551.
3. Skyler JS, Bakris GL, Bonifacio E, et al. Differentiation of diabetes by pathophysiology, natural history, and prognosis. *Diabetes* 2017;66:241-255.
4. Papanas N, Ziegler D. Risk factors and comorbidities in diabetic neuropathy: an update 2015. *Rev Diabet Stud* 2015;12(1-2):48-62
5. Sørensen BM, Houben AJ, Berendschot TT, et al. Prediabetes and type 2 diabetes are associated with generalized microvascular dysfunction: the Maastricht Study. *Circulation* 2016;134(18):1339-1352.
6. Greenman RL, Panasyuk S, Wang X, et al. Early changes in the skin microcirculation and muscle metabolism of the diabetic foot. *Lancet* 2005;366(9498):1711-1717.
7. Aguirre J, Schwarz M, Garzorzet N, al. Precision assessment of label-free psoriasis biomarkers with ultra-broadband optoacoustic mesoscopy. *Nat Biomed Eng* 2017;1:0068.
8. Ntziachristos V, Razansky D. Molecular imaging by means of multispectral optoacoustic tomography (MSOT). *Chem Rev* 2010;110(5):2783-2794.
9. Horton WB, Barrett EJ. Microvascular dysfunction in diabetes mellitus and cardiometabolic disease. *Endocr Rev* 2021;42(1):29-55.
10. Mulla IG, Anjankar A, Pratinidhi S, Agrawal SV, Gundpatil D, Lambe SD. Prediabetes: a benign intermediate stage or a risk factor in itself? *Cureus* 2024;16(6):e63186.
11. Ziegler D, Rathmann W, Dickhaus T, Meisinger C, Mielck A; KORA Study Group. Neuropathic pain in diabetes, prediabetes and normal glucose tolerance: the MONICA/KORA Augsburg Surveys S2 and S3. *Pain Med* 2009;10(2):393-400.

12. Hicks CW, Wang D, Matsushita K, Windham BG, Selvin E. Peripheral neuropathy and all-cause and cardiovascular mortality in U.S. adults : a prospective cohort study. *Ann Intern Med* 2021;174(2):167-174.
13. Kobayashi M, Zochodne DW. Diabetic neuropathy and the sensory neuron: New aspects of pathogenesis and their treatment implications. *J Diabetes Investig* 2018;9(6):1239-1254.
14. Hammes HP. Diabetic retinopathy: hyperglycaemia, oxidative stress and beyond. *Diabetologia* 2018;61(1):29-38.
15. Juster-Switlyk K, Smith AG. Updates in diabetic peripheral neuropathy. *F1000Res* 2016;5:738.
16. Xue T, Zhang X, Xing Y, et al. Advances about immunoinflammatory pathogenesis and treatment in diabetic peripheral neuropathy. *Front Pharmacol* 2021;12:748193.
17. Papanas N, Vinik AI, Ziegler D. Neuropathy in prediabetes: does the clock start ticking early? *Nat Rev Endocrinol.* 2011;7(11):682-690.
18. Røikjer J, Ejskjaer N. Diabetic peripheral neuropathy. *Handb Exp Pharmacol* 2022;274:309-328.
19. Herman WH, Kennedy L. Underdiagnosis of peripheral neuropathy in type 2 diabetes. *Diabetes Care* 2005;28(6):1480-1481.
20. Pop-Busui R, Boulton AJ, Feldman EL, et al. Diabetic neuropathy: a position statement by the American Diabetes Association. *Diabetes Care* 2017;40(1):136-154.
21. Selvarajah D, Kar D, Khunti K, et al. Diabetic peripheral neuropathy: advances in diagnosis and strategies for screening and early intervention. *Lancet Diabetes Endocrinol* 2019;7(12):938-948.
22. Petropoulos IN, Ponirakis G, Ferdousi M, et al. Corneal confocal microscopy: a biomarker for diabetic peripheral neuropathy. *Clin Ther* 2021;43(9):1457-1475.
23. Pafili K, Maltezos E, Papanas N. NC-stat for the diagnosis of diabetic polyneuropathy. *Expert Rev Med Devices* 2017;14(4):251-254.
24. Plevin S, Papanas N, Gatt A, Formosa C. Screening for diabetic peripheral neuropathy: subjective versus objective measures. *Int J Low Extrem Wounds.* Nov 3:15347346241295461. Online ahead of print.
25. Lauria G, Devigili G. Skin biopsy as a diagnostic tool in peripheral neuropathy. *Nat Clin Pract Neurol* 2007;3(10):546-557.

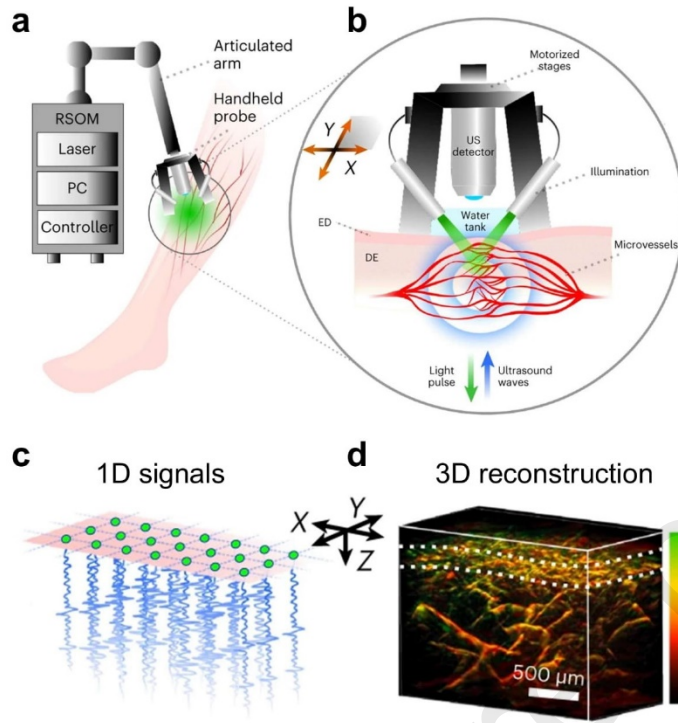
26. Bajwa A, Wesolowski R, Patel A, et al. Assessment of tissue perfusion in the lower limb: current methods and techniques under development. *Circ Cardiovasc Imaging* 2014;7(5):836-843.
27. Scheeren TWL, Schober P, Schwarte LA. Monitoring tissue oxygenation by near infrared spectroscopy (NIRS): background and current application. *J Clin Monit Comput* 2012;26(4):279-287.
28. Lu GB, Fei B. Medical hyperspectral imaging: a review. *J Biomed Opt* 2014;19:109-112.
29. Wilson SR, Greenbaum LD, Goldberg BB. Contrast-enhanced ultrasound: what is the evidence and what are the obstacles? *AJR Am J Roentgenol* 2009;193(1):55-60.
30. Ntziachristos V, Pleitez MA, Aime S, Brindle KM. Emerging technologies to image tissue metabolism. *Cell Metab* 2019;29(3):518-538.
31. Beard P. Biomedical photoacoustic imaging. *Interface Focus* 2011;1(4):602-631.
32. Masthoff M, Helfen A, Claussen J, et al. Use of multispectral optoacoustic tomography to diagnose vascular malformations. *JAMA Dermatol* 2018;154(12):1457-1462.
33. Yang H, Jüstel D, Prakash J, et al. Soft ultrasound priors in optoacoustic reconstruction: Improving clinical vascular imaging. *Photoacoustics* 2020;19:100172.
34. Yao J, Wang LV. Photoacoustic microscopy. *Laser Photon Rev* 2013;7(5):10.1002/lpor.201200060.
35. Oraevsky AA, Clingman B, Zalev J, Stavros AT, Yang WT, Parikh JR. Clinical optoacoustic imaging combined with ultrasound for coregistered functional and anatomical mapping of breast tumors. *Photoacoustics* 2018;12:30-45.
36. Schwarz M, Omar M, Buehler A, Aguirre J, Ntziachristos V. Implications of ultrasound frequency in optoacoustic mesoscopy of the skin. *IEEE Trans Med Imaging* 2015;34(2):672-677.
37. Taruttis A, Ntziachristos V. Advances in real-time multispectral optoacoustic imaging and its applications. *Nat Photonics* 2015;9:219-227.
38. Aguirre J, Schwarz M, Soliman D, Buehler A, Omar M, Ntziachristos V. Broadband mesoscopic optoacoustic tomography reveals skin layers. *Opt Lett* 2014;39(21):6297-6300.
39. Berezhnoi A, Aguirre J, Hindelang B, et al. Optical features of human skin revealed by optoacoustic mesoscopy in the visible and short-wave infrared regions. *Opt Lett* 2019;44(17):4119-4122.

40. Schwarz M, Buehler A, Aguirre J, Ntziachristos V. Three-dimensional multispectral optoacoustic mesoscopy reveals melanin and blood oxygenation in human skin in vivo. *J Biophotonics* 2016;9(1-2):55-60.
41. Karlas A, Pleitez MA, Aguirre J, Ntziachristos V. Optoacoustic imaging in endocrinology and metabolism. *Nat Rev Endocrinol* 2021;17(6):323-335.
42. Ntziachristos V. Going deeper than microscopy: the optical imaging frontier in biology. *Nat Methods* 2010;7(8):603-614.
43. Omar M, Soliman D, Gateau J, Ntziachristos V. Ultrawideband reflection-mode optoacoustic mesoscopy. *Opt Lett* 2014;39(13):3911-3914.
44. Omar M, Gateau J, Ntziachristos V. Raster-scan optoacoustic mesoscopy in the 25-125 MHz range. *Opt Lett* 2013;38(14):2472-2474.
45. Regensburger AP, Brown E, Krönke G, Waldner MJ, Knieling F. Optoacoustic imaging in inflammation. *Biomedicine* 2021;9(5):483.
46. Li X, Yew YW, Vinod Ram K, et al. Structural and functional imaging of psoriasis for severity assessment and quantitative monitoring of treatment response using high-resolution optoacoustic imaging. *Photoacoustics* 2024;38:100611.
47. Li X, Moothanchery M, Kwa CY, et al. Multispectral raster-scanning optoacoustic mesoscopy differentiate lesional from non-lesional atopic dermatitis skin using structural and functional imaging markers. *Photoacoustics* 2022;28:100399.
48. Nau T, Schönmann C, Hindelang B, et al. Raster-scanning optoacoustic mesoscopy biomarkers for atopic dermatitis skin lesions. *Photoacoustics* 2023;31:100513.
49. Omar M, Schwarz M, Soliman D, Symvoulidis P, Ntziachristos V. Pushing the optical imaging limits of cancer with multi-frequency-band raster-scan optoacoustic mesoscopy (RSOM). *Neoplasia* 2015;17(2):208-214.
50. He H, Schönmann C, Schwarz M, et al. Fast raster-scan optoacoustic mesoscopy enables assessment of human melanoma microvasculature in vivo. *Nat Commun* 2022;13(1):2803.
51. He H, Fasoula NA, Karlas A, et al. Opening a window to skin biomarkers for diabetes stage with optoacoustic mesoscopy. *Light Sci Appl* 2023;12(1):231.
52. Karlas A, Katsouli N, Fasoula NA, et al. Dermal features derived from optoacoustic tomograms via machine learning correlate microangiopathy phenotypes with diabetes stage. *Nat Biomed Eng* 2023;7(12):1667-1682.
53. Karlas A, Masthoff M, Kallmayer M, et al. Multispectral optoacoustic tomography of peripheral arterial disease based on muscle hemoglobin gradients—a pilot clinical study. *Ann Transl Med* 2021;9(1):36.

54. Diot G, Metz S, Noske A, et al. Multispectral optoacoustic tomography (MSOT) of human breast cancer. *Clin Cancer Res* 2017;23(22):6912-6922.
55. Menezes GLG, Pijnappel RM, Meeuwis C, et al. downgrading of breast masses suspicious for cancer by using optoacoustic breast imaging. *Radiology* 2018;288(2):355-365.
56. Dima A, Ntziachristos V. In-vivo handheld optoacoustic tomography of the human thyroid. *Photoacoustics* 2016;4(2):65-69.
57. Knieling F, Neufert C, Hartmann A, et al. Multispectral optoacoustic tomography for assessment of Crohn's disease activity. *N Engl J Med* 2017;376(13):1292-1294.
58. Omar M, Aguirre J, Ntziachristos V. Optoacoustic mesoscopy for biomedicine. *Nat Biomed Eng* 2019;3(5):354-370.
59. Attia ABE, Balasundaram G, Moothanchery M, et al. A review of clinical photoacoustic imaging: Current and future trends. *Photoacoustics* 2019;16:100144.
60. Jeon S, Kim J, Lee D, Baik JW, Kim C. Review on practical photoacoustic microscopy. *Photoacoustics*. 2019;15:100141.
61. Jin T, Guo H, Jiang H, Ke B, Xi L. Portable optical resolution photoacoustic microscopy (pORPAM) for human oral imaging. *Opt Lett* 2017;42(21):4434-4437.
62. Wong TT, Zhang R, Hai P, et al. Fast label-free multilayered histology-like imaging of human breast cancer by photoacoustic microscopy. *Sci Adv* 2017;3(5): e1602168.
63. Yagihashi S, Mizukami H, Sugimoto K. Mechanism of diabetic neuropathy: Where are we now and where to go? *J Diabetes Investig* 2011;2(1):18-32.
64. Shi Y, Vanhoutte PM. Macro- and microvascular endothelial dysfunction in diabetes. *J Diabetes* 2017;9(5):434-449.
65. Clyne AM. Endothelial response to glucose: dysfunction, metabolism, and transport. *Biochem Soc Trans* 2021;49(1):313-325.
66. McMillan DE. Deterioration of the microcirculation in diabetes. *Diabetes* 1975;24(10):944-957.
67. Forbes JM, Cooper ME. Mechanisms of diabetic complications. *Physiol Rev* 2013;93(1):137-188.
68. Cypress M, Tomky D. Microvascular complications of diabetes. *Nurs Clin North Am* 2006;41(4):719-ix.
69. Avram R, Olgin JE, Kuhar P, et al. A digital biomarker of diabetes from smartphone-based vascular signals. *Nat Med* 2020;26(10):1576-1582.
70. Yoon HS, Baik SH, Oh CH. Quantitative measurement of desquamation and skin elasticity in diabetic patients. *Skin Res Technol* 2002;8(4):250-254.
71. Hsiu H, Hu HF, Tsai HC. Differences in laser-Doppler indices between skin-surface measurement sites in subjects with diabetes. *Microvasc Res* 2018;115:1-7.
72. Ntziachristos V. Addressing unmet clinical need with optoacoustic imaging. *Nat Rev Bioeng* 2025. Epub ahead of print.

73. Ghazaryan A, Omar M, Tserevelakis GJ, Ntziachristos V. Optoacoustic detection of tissue glycation. *Biomed Opt Express* 2015;6(9):3149-3156.
74. Lyssenko V, Vaag A. Genetics of diabetes-associated microvascular complications. *Diabetologia* 2023;66(9):1601-1613.

Journal Pre-proofs



	Macroscopy [37, 41]	Mesoscopy (Raster Scan Optoacoustic Mesoscopy) [41, 43, 58, 59]	Microscopy [34, 60, 61]
<i>Typical wavelength range</i>	650-1100 nm	400-900 nm	400-700 nm
<i>Typical US transducer frequency range</i>	0.1-10 MHz	10-50 MHz (UWB-RSOM: ≤200MHz)	>30 MHz
<i>Typical depth</i>	1-4 cm	1-10 mm	0.1-2 mm (OR-OptAM: <0.2mm)
<i>Typical resolution</i>	100-300 μm	10-100 μm	5-30 μm (OR-OptAM: <1 μm)
<i>Common applications</i>	cardiovascular disease [53] breast cancer imaging [54, 55] thyroid imaging [56] Crohn's disease [57]	diabetes mellitus [51, 52] melanoma [49, 50] psoriasis [8]	microangiography in cancer biology [62] histological examination [62]

nm, nanometres; US, ultrasound; MHz, megahertz; UWB-RSOM, ultra wide band Raster Scan Mesoscopy; cm, centimetres; mm, millimetres; μm , micrometres; DV OR-PAM, dual view optical resolution photoacoustic microscopy

Table 1. Optoacoustic imaging modalities.

Authors	Study population	Image acquisition	Main Findings
He et al. ⁵¹	143 subjects: 95 DM subjects 48 healthy volunteers	UWB-RSOM laser wavelength: 532 nm US transducer: 10 – 120 MHz 2 symmetric 4x2 mm ² regions over the pretibial area of the distal lower limbs	<ol style="list-style-type: none"> 1. As diabetic microvascular complications develop, the vascular density in the dermal layer decreases and the epidermis becomes thinner and less light absorbing. 2. RSOM able to classify participants with DM based on skin microvasculature changes. (density of vessels <40 µm in diameter was the most indicative marker of presence of diabetic microvascular complications). 3. Small vessels number can be used as differentiating biomarker among healthy subjects and DM subjects with microvascular complications.
Karlas et al. ⁵²	115 subjects: 75 DM subjects 40 healthy volunteers (199 RSOM images)	UWB-RSOM laser wavelength: 532 nm US transducer: 10 – 120 MHz 4x2 mm ² region, distal anterolateral area of the dominant leg (~15 cm above ankle)	<ol style="list-style-type: none"> 1. RSOM features that belong to the mesoscale, which describes the morphology and organisation of the microvascular network, are more sensitive to DM and presence of diabetic microvascular complications. 2. microangiopathy score: (comprising RSOM imaging features) was found to be higher for DM subjects than that of healthy volunteers (p<0.001)

UWB-RSOM, ultra-wide band Raster Scan Optoacoustic Mesoscopy; nm, nanometres; US, ultrasound; MHz, megahertz; mm², square millimetres; RSOM, Raster Scan Optoacoustic Mesoscopy; µm, micrometres; cm, centimetres; DM, diabetes mellitus

Table 2. Clinical studies of Raster Scan Optoacoustic Mesoscopy in DM.

Journal Pre-proofs

DECLARATION OF INTEREST STATEMENT

Conflicts of interest: **Dimitrios Pantazopoulos** has been supported by Technical University of Munich. **Evanthia Gouveri** has attended conferences sponsored by Berlin-Chemie, Sanofi, AstraZeneca, Novo Nordisk, Lilly and Boehringer Ingelheim; received speaker honoraria by Boehringer-Ingelheim, Sanofi and Menarini. **Nikolaos Papanas** has been an advisory board member of Astra-Zeneca, Bayer, Boehringer Ingelheim, Menarini, MSD, Novo Nordisk, Pfizer, Takeda and TrigoCare International; has participated in sponsored studies by Astra-Zeneca, Eli-Lilly, GSK, MSD, Novo Nordisk, Novartis and Sanofi-Aventis; has received honoraria as a speaker for Astra-Zeneca, Bayer, Boehringer Ingelheim, Eli-Lilly, Elpen, Menarini, MSD, Mylan, Novo Nordisk, Pfizer, Sanofi-Aventis and Vianex; and has attended conferences sponsored by TrigoCare International, Eli-Lilly, Galenica, Menarini, Novo Nordisk, Pfizer and Sanofi-Aventis. **Vasilis Ntziachristos** is a founder and equity holder of iThera Medical GmbH, Spear UG, sThesis GmbH, I3 Inc and Maurus OY.

Acknowledgments: This project has received funding from the European Union's Horizon 2020 research and innovation programme under grant agreement No 101017802 (OPTOMICS).